Endoplasmic Reticulum Stress in the Proapoptotic Action of Edelfosine in Solid Tumor Cells

Teresa Nieto-Miguel,[1] Rosalba I. Fonteriz,[3] Laura Vay,[3] Consuelo Gajate,[1,2] Silvia López-Hernández,[1] and Faustino Mollinedo[1]

[1]Centro de Investigación del Cáncer, Instituto de Biología Molecular y Celular del Cáncer, Consejo Superior de Investigaciones Científicas-Universidad de Salamanca; [2]Unidad de Investigación, Hospital Universitario de Salamanca, Campus Miguel de Unamuno, Salamanca, Spain; and [3]Departamento de Bioquímica y Biología Molecular y Fisiología, Instituto de Biología y Genética Molecular, Facultad de Medicina, Universidad de Valladolid-Consejo Superior de Investigaciones Científicas, Valladolid, Spain

Abstract

The endoplasmic reticulum (ER) has been posited as a potential anticancer target. The synthetic antitumor alkyl-lysophospholipid analogue edelfosine accumulates in the ER of solid tumor cells. This ER accumulation of the drug leads to the inhibition of phosphatidylcholine and protein synthesis, G_2-M arrest, depletion of ER-stored Ca^{2+}, Bax up-regulation and activation, transcriptional factor growth arrest and DNA damage–inducible gene 153 up-regulation, caspase-4 and caspase-8 activation, and eventually to apoptosis. Edelfosine prompted ER stress apoptotic signaling, but not the survival unfolded protein response. Edelfosine also induced persistent c-*Jun* NH_2-terminal kinase (JNK) activation. Gene transfer–mediated overexpression of apoptosis signal–regulating kinase 1, which plays a crucial role in ER stress, enhanced edelfosine-induced JNK activation and apoptosis. Inhibition of JNK, caspase-4, or caspase-8 activation diminished edelfosine-induced apoptosis. Edelfosine treatment led to the generation of the p20 caspase-8 cleavage fragment of BAP31, directing proapoptotic signals between the ER and the mitochondria. *bax*$^{-/-}$*bak*$^{-/-}$ double-knockout cells fail to undergo edelfosine-induced ER-stored Ca^{2+} release and apoptosis. Wild-type and *bax*$^{-/-}$*bak*$^{-/-}$ cells showed similar patterns of phosphatidylcholine and protein synthesis inhibition, despite their differences in drug sensitivity. Thus, edelfosine-induced apoptosis is dependent on Bax/Bak-mediated ER-stored Ca^{2+} release, but phosphatidylcholine and protein synthesis inhibition is not critical. Transfection-enforced expression of Bcl-X_L, which localizes specifically in mitochondria, prevented apoptosis without inhibiting ER-stored Ca^{2+} release. These data reveal that edelfosine induces an ER stress response in solid tumor cells, providing novel insights into the edelfosine-mediated antitumor activity. Our data also indicate that mitochondria are indispensable for this edelfosine-induced cell death initiated by ER stress. [Cancer Res 2007;67(21):10368–78]

Introduction

Synthetic alkyl-lysophospholipid analogues (ALP), from which 1-*O*-octadecyl-2-*O*-methyl-*rac*-glycero-3-phosphocholine (ET-18-OCH_3, edelfosine) is their prototypic compound, represent a promising class of oral anticancer drugs that do not target the DNA (1–3). Recent *in vitro* and *in vivo* data (4, 5) have prompted renewed interest in the study of their antitumor properties and underlying mechanisms. The antitumor action of edelfosine relies on its ability to induce apoptosis in a wide spectrum of tumor cells (1, 6), involving c-*Jun* NH_2-terminal kinase (JNK) persistent activation (7) and mitochondria (8). Edelfosine induces a rapid apoptotic response in leukemic cells through coclustering of Fas/CD95 death receptor and lipid rafts, independently of Fas/CD95 ligand (5, 9, 10). Edelfosine targets mainly lipid rafts in hematologic malignancies and the endoplasmic reticulum (ER) in solid tumor cells (10, 11), hence showing different targets in distinct tumor cell types.

ER has been recently shown to modulate cell death. When the functions of the ER are severely impaired, the organism protects itself by getting rid of the damaged cells through apoptosis. ER is composed of a system of connected membranous tubules and vesicles along which protein and phospholipid synthesis occur and intracellular calcium levels are regulated. Thus, disruption in Ca^{2+} homeostasis, inhibition of protein glycosylation, accumulation of misfolded proteins, and inhibition of phosphatidylcholine could all challenge the function of the ER-Golgi network resulting in ER stress, and excessive ER stress leads to apoptosis (12, 13). The ER stress response includes: induction of the transcription factor CCAAT/enhancer binding protein–homologous protein (CHOP), a.k.a. growth arrest and DNA damage–inducible gene 153 (*GADD153*), activation of JNK through the apoptosis signal–regulating kinase 1 (ASK1), and activation of the ER-localized caspase-12 in murine systems or caspase-4 in human cells (12–15).

Some anticancer chemotherapeutic agents have been shown to induce ER stress, including the proteasome inhibitor bortezomib (16), the Hsp90 inhibitors, geldanamycin and 17-allyl-amino-geldanamycin (17), cisplatin (18), and cannabinoids (19). However, these agents target ER-mediated processes rather than the ER itself, leading indirectly to ER stress. We have recently found that edelfosine accumulates predominantly at the ER in a number of solid tumor cells (11). Now, we report here that the accumulation of edelfosine at the ER of solid tumor cells alters ER functions, leading to ER stress and eventually to apoptosis.

Materials and Methods

Reagents. Edelfosine (INKEYSA) was prepared as a 1 mmol/L stock solution as previously described (1). Caspase-4 inhibitor z-LEVD-fmk was

Note: Supplementary data for this article are available at Cancer Research Online (http://cancerres.aacrjournals.org/).

Requests for reprints: Faustino Mollinedo, Centro de Investigación del Cáncer, Instituto de Biología Molecular y Celular del Cáncer, Consejo Superior de Investigaciones Científicas-Universidad de Salamanca, Campus Miguel de Unamuno, E-37007 Salamanca, Spain. Phone: 34-923-294806; Fax: 34-923-294795; E-mail: fmollin@usal.es.

doi:10.1158/0008-5472.CAN-07-0278

from Alexis Biochemicals. Caspase-8 inhibitor z-IETD-fmk and JNK inhibitor SP600125 were from Calbiochem. Fura-2 acetoxymethyl ester (fura-2/AM) was from Molecular Probes. Cycloheximide, tunicamycin, and histamine were from Sigma.

Cell culture and *bcl-x_L* transfection. Human cells were grown in DMEM (HeLa) or RPMI 1640 (A549) supplemented with 10% heat-inactivated FCS, 2 mmol/L of L-glutamine, 100 units/mL penicillin, and 100 μg/mL of streptomycin at 37°C in 5% CO_2 humidified air. HeLa cells ($1–2 \times 10^5$) were transfected with 2 μg of pSFFV-*bcl-x_L* or pSFFV-Neo expression vector (1), using Lipofectin reagent (Life Technologies). Transfected clones were selected by growth in the presence of 500 μg/mL of G418 (Sigma) and monitored by Western blotting using the 2H12 anti–29 kDa Bcl-X_L monoclonal antibody (BD Biosciences PharMingen).

Wild-type and *bax*$^{-/-}$*bak*$^{-/-}$ double-knockout (DKO) SV40-transformed mouse embryo fibroblasts (MEFs), as well as single knockout *bax*$^{-/-}$ or *bak*$^{-/-}$ MEFs, kindly provided by S.J. Korsmeyer (Dana-Farber Cancer Institute, Boston, MA; ref. 20), were cultured in DMEM supplemented with 10% FCS, 2 mmol/L of L-glutamine, 0.1 mmol/L of nonessential amino acids, 50 μmol/L of β-mercaptoethanol, 100 units/mL of penicillin, and 100 μg/mL of streptomycin.

ASK1 transfection. HeLa cells (5×10^5) were seeded and transfected with 6 μg of ASK1 wild-type (pcDNA3.1-ASK1), kindly provided by H. Ichijo (University of Tokyo, Japan), or with empty pcDNA3.1 vector (Invitrogen), using the cationic polymer transfection reagent jetPEI (Qbiogene). Transfected clones were selected by growth in the presence of 500 μg/mL of G418 and monitored by Western blotting using an anti–155 kDa ASK1 rabbit polyclonal antibody (dilution 1:500; eBioscience).

Apoptosis and cell cycle analysis. Cell cycle analysis and quantitation of apoptotic cells (hypodiploidy) were determined by flow cytometry as previously described (21).

Phosphatidylcholine biosynthesis. Cells ($2–3 \times 10^6$) were washed with PBS and incubated with 1 μCi/mL of [methyl-^{14}C]choline chloride (Amersham Biosciences) for 30 min in FCS-free culture medium. Labeled cells were washed thrice with PBS, resuspended in the presence or absence of edelfosine in complete culture medium for the indicated times, and analyzed for phosphatidylcholine synthesis as described previously (11). Radioactive lipids were visualized using a Fujifilm BAS-MS PhosphorImager and identified using internal controls. Spots corresponding to labeled phosphatidylcholine were quantitated by laser densitometry.

Protein synthesis. Cells ($2–2.5 \times 10^6$) were washed with PBS and incubated in FCS- and methionine-free medium for 15 to 20 min. Before labeling with 0.5 μCi/mL of [^{35}S]methionine (Amersham) for the indicated times, cells were incubated in the absence (negative control) or presence of 10 μmol/L of edelfosine or 75 μmol/L of cycloheximide (positive control). After one wash with PBS/2% bovine serum albumin and twice with PBS, cells were lysed in 25 mmol/L of Hepes (pH 7.7), 0.3 mol/L of NaCl, 1.5 mmol/L of $MgCl_2$, 0.2 mmol/L of EDTA, 0.1% Triton X-100, 20 mmol/L of β-glycerophosphate, and 0.1 mmol/L of sodium orthovanadate for 20 to 30 min at 4°C. Proteins were precipitated with trichloroacetic acid. After centrifugation, samples were resuspended in 100 μL of Tris-HCl at 0.5 mol/L (pH 9.0), and radioactivity incorporation into precipitated proteins was measured with a scintillation counter.

RT-PCR. Five micrograms of total RNA was primed with random hexamers and reverse-transcribed with SuperScript III reverse transcriptase (Invitrogen) in a 20 μL volume. The generated cDNA was amplified by using primers for human *gadd153/chop* (forward 5′-CATTGCCTTTCTCTTCGGAC-3′ and reverse 5′-GCCACTTTCCTTTCATTCTCC-3′), and *β-actin* (forward 5′-CTGTCTGGCGGCACCACCAT-3′ and reverse 5′-GCAACTAAGTCATAGTCCGC-3′). The PCR profile was as follows: 95°C for 30 s; 56°C (*gadd153/chop*) or 65°C (*β-actin*) for 30 s; 72°C for 90 s. After 30 cycles, shown to be at the linear phase of amplification, the expected PCR products (379 bp for *gadd153/chop*, and 254 bp for *β-actin*) were size-fractionated onto 2% agarose gel and stained with ethidium bromide.

Solid phase JNK assay. A fusion protein between glutathione S-transferase and c-*Jun* (amino acids 1–223) was used as a substrate for JNK activity as described previously (22).

Western blot. Cells ($4–5 \times 10^6$) were lysed with 60 μL of 25 mmol/L Hepes (pH 7.7), 0.3 mol/L of NaCl, 1.5 mmol/L of $MgCl_2$, 0.2 mmol/L of EDTA, 0.1% Triton X-100, 20 mmol/L of β-glycerophosphate, 0.1 mmol/L of sodium orthovanadate supplemented with protease inhibitors (1 mmol/L phenylmethylsulfonyl fluoride, 20 μg/mL aprotinin, 20 μg/mL leupeptin). Fifty micrograms of proteins were run on SDS-polyacrylamide gels, transferred to nitrocellulose filters, blocked with 5% (w/v) power defatted milk in TBST [50 mmol/L Tris-HCl (pH 8.0), 150 mmol/L NaCl, and 0.1% Tween 20] for 90 min at room temperature, and incubated for 1 h at room temperature or overnight at 4°C with specific antibodies: R-20 anti–30 kDa CHOP/GADD153 (1:250 dilution) and H-129 anti–78 kDa Grp78/BiP (1:500 dilution) rabbit polyclonal antibodies, N-15 anti–50 kDa caspase-4 (1:250 dilution) goat polyclonal antibody that also detects the p20 subunit, C-20 anti–55 kDa caspase-8 (1:500 dilution) goat polyclonal antibody that also recognizes the p20 subunit, C-15 anti–28 kDa BAP31 (1:500 dilution) goat polyclonal antibody (Santa Cruz Biotechnology); CM1 anti–18 kDa active caspase-3 (1:5,000 dilution) rabbit polyclonal antibody, and 2H12 anti–29 kDa Bcl-X_L (1:500 dilution), 6A7 anti–21 kDa Bax (1:500 dilution), and G317-2 anti–24 kDa Bak (1:500 dilution) monoclonal antibodies (BD Biosciences PharMingen); AC-15 anti–42 kDa β-actin (1:5,000 dilution) monoclonal antibody (Sigma); and anti–40 kDa eukaryotic initiation factor (eIF2α; 1:1,000 dilution) rabbit polyclonal antibody and 119A11 anti–40 kDa phosphorylated eIF2α (Ser^{51}; 1:1,000 dilution) rabbit monoclonal antibody (Cell Signaling Technology). Signals were developed using an enhanced chemiluminescence detection kit (Amersham).

Flow cytometry detection of intracellular proteins. Cells were fixed and permeabilized by means of the Fix & Perm cell permeabilization kit (CALTAG Laboratories) following the manufacturer's instructions. Cells were then incubated with monoclonal antibodies against the active forms of Bax (clone 6A7; BD Biosciences PharMingen) and Bak (clone Ab-1; Calbiochem) at 1:50 dilution in PBS for 15 min at room temperature, washed with PBS, stained for 15 min with Cy2-conjugated antimouse IgG at 1:50 dilution (Jackson ImmunoResearch Laboratories, Inc.), and analyzed in a Becton Dickinson fluorescence-activated cell sorting (FACS)Calibur flow cytometer. Data are shown as the mean fluorescence intensity, which was corrected for unspecific staining by subtracting the fluorescence of cells stained with negative controls. P3X63 myeloma culture supernatant, kindly provided by F. Sánchez-Madrid (Hospital de La Princesa, Madrid, Spain), and an isotype-matched nonrelevant IgG monoclonal antibody were used as negative controls, leading to virtually identical background values.

Single cell calcium measurement. Cells were loaded with the cell-permeable fura-2/AM by incubation in standard medium (145 mmol/L NaCl, 5 mmol/L KCl, 1 mmol/L $CaCl_2$, 1 mmol/L $MgCl_2$, 10 mmol/L Hepes; pH 7.4) for 40 min at room temperature. Cells were then washed with standard medium for 10 min at room temperature and mounted in a cell chamber on the stage of a Zeiss Axiovert 200 microscope under continuous perfusion. Single cell fluorescence was excited at 340 and 380 nm using a Cairn monochromator (100 ms excitation at each wavelength every 2 s) and images of the fluorescence emitted above 500 nm obtained with a 40× Fluar objective were recorded by a Hamamatsu ORCA-ER camera (Hamamatsu, Japan). Single cell fluorescence records were rationed and calibrated into cytoplasmic free Ca^{2+} concentration values off-line as described previously (23) using Metafluor program (Universal Imaging). Experiments were done at 37°C using an on-line heater from Harvar Apparatus. Cells were perfused with standard medium containing 1 mmol/L of $CaCl_2$ or with Ca^{2+}-lacking medium (0 mmol/L Ca^{2+}) that contained 0.5 mmol/L of EGTA in substitution of Ca^{2+}. Edelfosine and histamine were added to the perfusion medium at the indicated final concentrations from stock solutions. Aqueous stock solutions of 10 and 1 mmol/L edelfosine were used. Different solutions were changed by means of a multichannel perfusion system.

Results

Edelfosine inhibits phosphatidylcholine and protein synthesis. We have recently found that the edelfosine fluorescent analogue PTE-edelfosine, which has been previously shown to preserve the apoptotic features of the parental edelfosine in a number of different cell types, is located in the ER of distinct cancer cell lines derived from human malignant solid tumors,

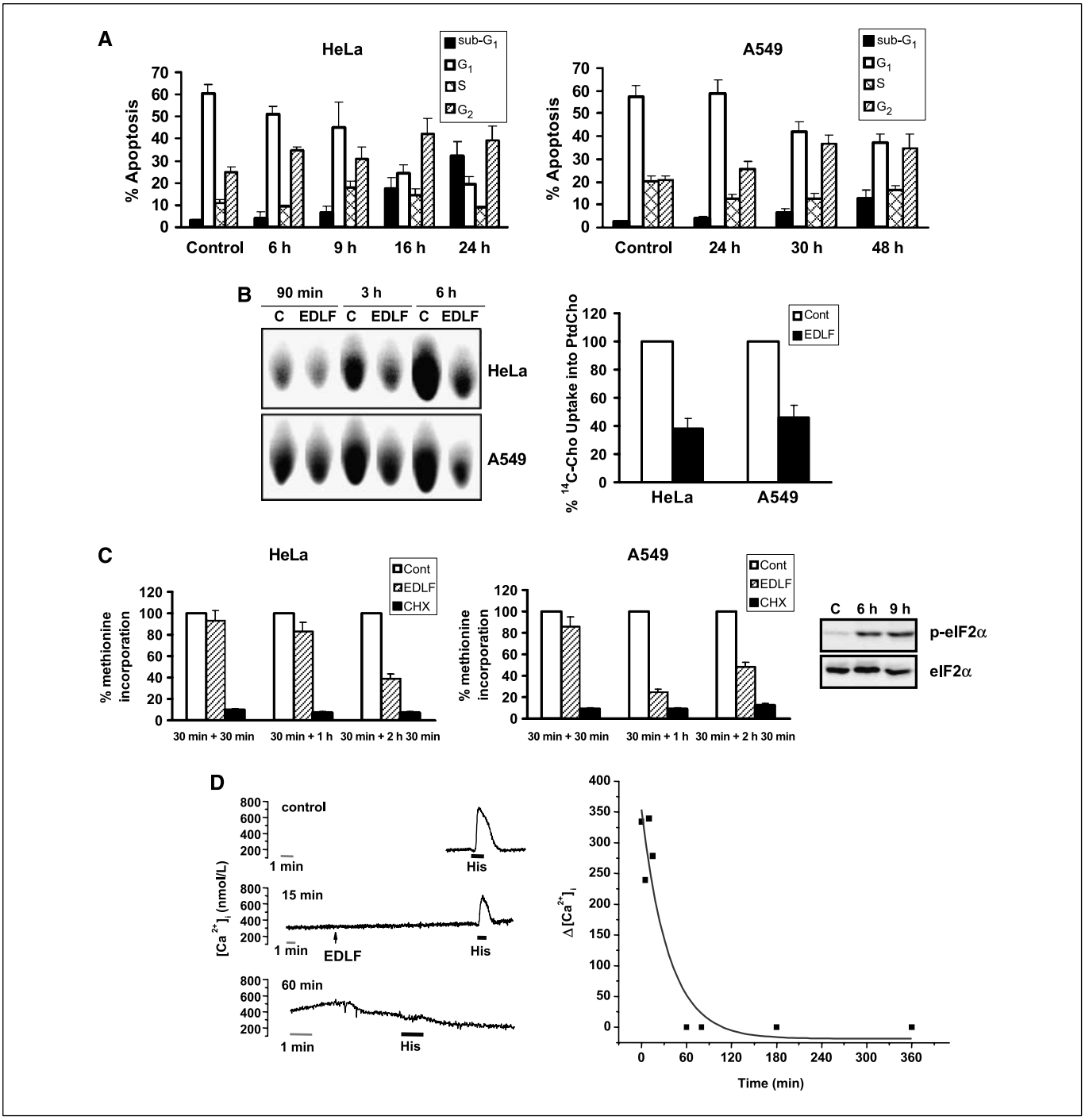

Figure 1. Effects of edelfosine on cell cycle, apoptosis, and ER homeostasis. *A,* cells were treated with 10 μmol/L of edelfosine for the indicated times and the proportion of cells in each phase of cell cycle was quantitated by flow cytometry. The sub-G_1 region represents apoptotic cells. Untreated control cells were run in parallel. *Columns,* means; *bars,* SE (n = 4). *B, left,* [^{14}C]choline-labeled cells were grown in the absence (*C*) or presence of 10 μmol/L of edelfosine (*EDLF*) for the indicated times. Image shows phosphatidylcholine corresponding TLC spots visualized by phosphorimaging and is representative of three independent experiments. *Right,* percentage of [^{14}C]choline (*Cho*) incorporation into phosphatidylcholine (*PtdCho*) in HeLa cells treated with 10 μmol/L of edelfosine for 6 h (*EDLF*) with respect to untreated control HeLa cells (*Cont*; 100%). *Columns,* means; *bars,* SE (n = 3). *C, left,* HeLa and A549 cells were preincubated for 30 min in the absence (*Cont*) or presence of edelfosine (*EDLF*) or cycloheximide (*CHX*), and then [^{35}S]methionine was added to the culture medium for the indicated times. Percentages of newly synthesized labeled proteins in drug-treated cells with respect to untreated samples (100%). *Columns,* means; *bars,* SE (n = 3). *Right,* HeLa cells were incubated in the absence (*C*) or presence of 10 μmol/L of edelfosine for the indicated times and analyzed for eIF2α phosphorylation by immunoblotting, using a specific anti–phosphorylated eIF2α antibody. Immunoblotting for eIF2α was used as a control for protein loading. Representative of three independent experiments. *D, left,* cytosolic free calcium concentration was measured in fura-2/AM–loaded HeLa cells. Calcium release from intracellular stores was elicited by 1-min incubation with 100 μmol/L of histamine (*His*) in 0 Ca^{2+} medium. When indicated (*arrow*), medium containing 10 μmol/L of edelfosine was perfused for 15 min (*middle*). *Bottom,* cells incubated for 60 min in standard medium containing 10 μmol/L of edelfosine. During the experiment, cells were perfused with 0 Ca^{2+} medium and calcium release from intracellular stores was elicited by the addition of 100 μmol/L of histamine. *Top,* cells in the absence of edelfosine (*control*). Mean values of >100 cells from four different experiments. *Right,* plot of increments in calcium release from intracellular stores versus incubation time with 10 μmol/L of edelfosine in HeLa cells. Best fit to first-order exponential decay is represented.

including human cervix epitheloid carcinoma HeLa and human lung carcinoma A549 cells (11). Owing to the accumulation of edelfosine in the ER, we investigated whether an alteration in ER homeostasis could be involved in the antitumor action of this drug.

Edelfosine induced apoptosis in HeLa and A549 cells after a rather long incubation time following a cell cycle arrest in G_2-M (Fig. 1*A*). Because ER is responsible for the synthesis of proteins and lipids, we first analyzed the effect of the drug on both phosphatidylcholine and protein synthesis. Cells were incubated with [^{14}C]choline for 30 min, followed by exhaustive washing, and incubation in the absence or presence of edelfosine for different times, thus avoiding any effects that edelfosine might have on the uptake of choline into the cells (24). We found that edelfosine inhibited [^{14}C]choline incorporation into the phosphatidylcholine pool in both HeLa and A549 cells (Fig. 1*B*). These results are in agreement with previous studies showing inhibition of phosphatidylcholine biosynthesis by this drug at the phosphocholine cytdilyltransferase (CCT) step (25). Edelfosine also inhibited protein synthesis in both HeLa and A549 cells (Fig. 1*C*). Cycloheximide, used at a concentration that prevented protein synthesis (Fig. 1*C*), induced a slight apoptotic response which was increased following its combination with edelfosine

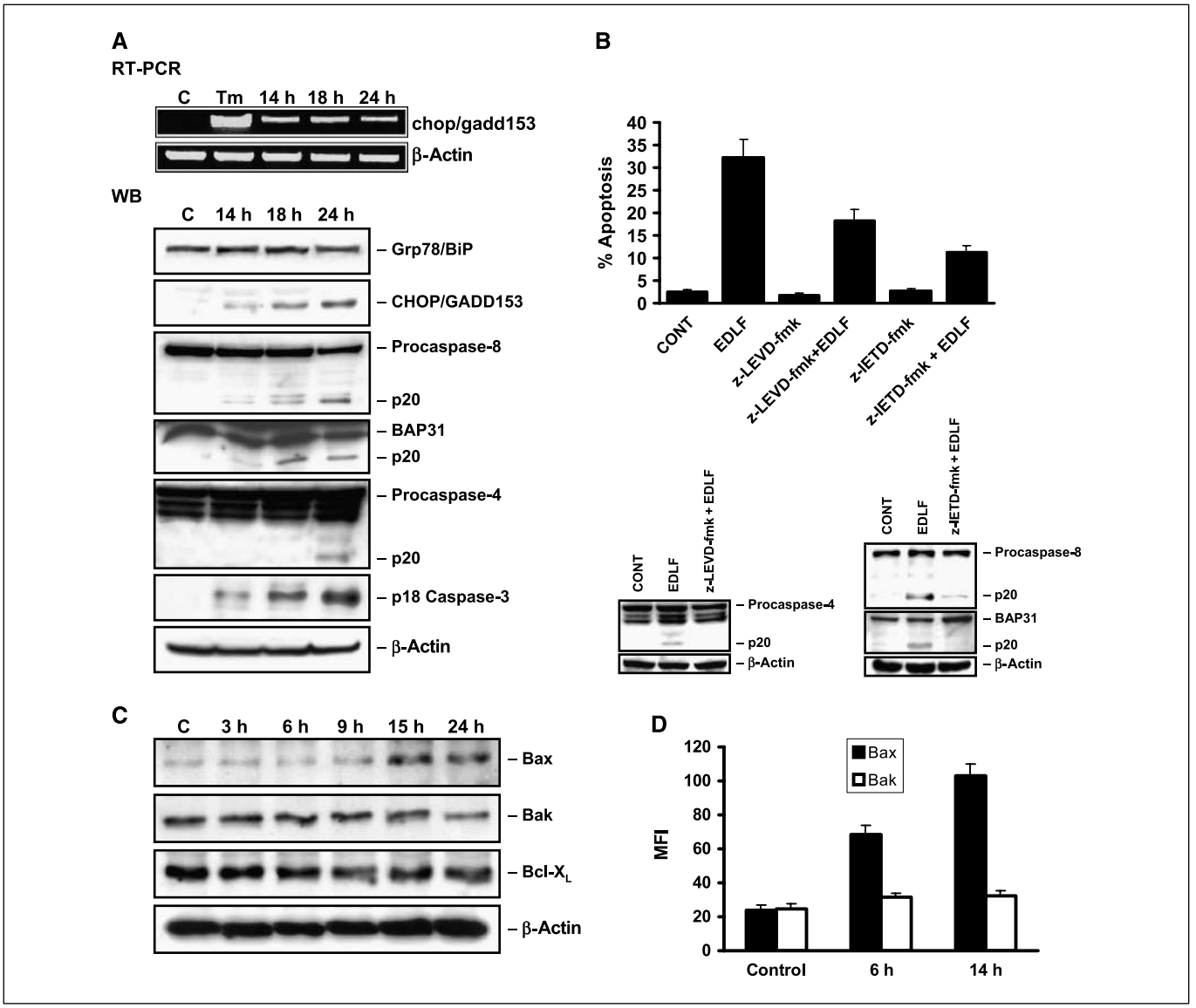

Figure 2. ER stress in edelfosine-treated HeLa cells. *A, top,* cells were untreated (*C*) or treated with 10 μmol/L edelfosine for the indicated times and *chop/gadd153* gene expression was assessed by semiquantitative RT-PCR. Cells treated with 25 μmol/L of tunicamycin (*Tm*) for 3 h were used as a positive control. PCR amplification of *β-actin* was used as an internal control. Representative of three experiments. *Bottom,* cells untreated (*C*) or treated with 10 μmol/L edelfosine for the indicated times were analyzed by Western blot (*WB*) using specific antibodies for the indicated proteins. *B,* cells were preincubated without or with 20 μmol/L of z-LEVD-fmk or 100 μmol/L of z-IETD-fmk for 1 h, and then incubated in the absence or presence of 10 μmol/L of edelfosine (*EDLF*) for 24 h, and analyzed by flow cytometry to evaluate apoptosis (*top*) or by immunoblotting using specific antibodies (*bottom*). Untreated control cells (*CONT*) were run in parallel. *C,* cells untreated (*C*) or treated with 10 μmol/L of edelfosine for the indicated times were analyzed by immunoblotting using specific antibodies for the indicated proteins. *D,* conformational changes in Bax and Bak were determined as described in Materials and Methods in untreated control cells and following treatment with 10 μmol/L of edelfosine for the indicated times. β-Actin was used as a loading control in Western blot analyses. *B* (*top*) and *D, columns,* means; *bars,* SE (n = 3). Blots are representative of three independent experiments.

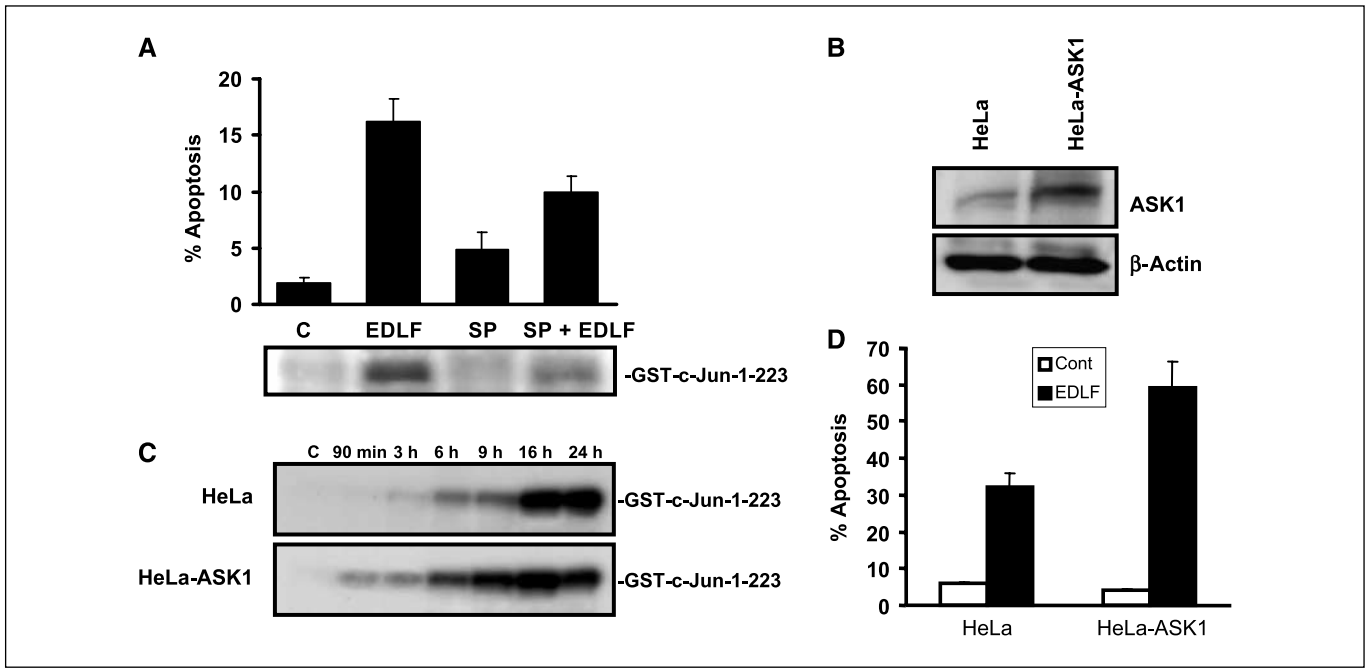

Figure 3. Edelfosine-induced apoptosis is mediated by ASK1-JNK activation in HeLa cells. *A,* cells were pretreated with 20 μmol/L of SP600125 (*SP*) for 1 h, and then incubated in the absence or presence of 10 μmol/L of edelfosine (*EDLF*) for 16 h, and analyzed for apoptosis and JNK activation. The migration position of GST-c-Jun-1-223 is indicated. Untreated control cells (*C*) were run in parallel. *Columns,* means; *bars,* SE (n = 3). *B,* ASK1 protein expression was analyzed by SDS-PAGE of 100 μg of cell extract protein and immunoblotting. β-Actin was used as a control for protein loading. *C,* cells were untreated (*C*) or treated with 10 μmol/L of edelfosine for different times and assayed for JNK activation. The migration position of GST-c-Jun-1-223 is indicated. Representative of three experiments. *D,* cells were treated with 10 μmol/L of edelfosine (*EDLF*) for 24 h and analyzed for apoptosis. Untreated control cells (*Cont*) were run in parallel. *Columns,* means; *bars,* SE (n = 3).

(Supplementary Fig. S1). Edelfosine induced the phosphorylation of eIF2α (Fig. 1*C, right*), thereby mediating translational repression (26). Protein synthesis inhibition prevents the constant accumulation of newly synthesized proteins into the ER when ER itself and/or protein folding conditions are compromised. Our data indicate that edelfosine affects both phospholipid and protein homeostasis.

Edelfosine induces the release of ER-stored Ca^{2+}. Because ER is the main Ca^{2+} cellular store, we analyzed the effect of edelfosine on ER calcium release. Treatment of HeLa cells with edelfosine for 15 min reduced histamine-induced calcium release from intracellular stores by ~45% (integral of calcium wave; Fig. 1*D, left*). A 60-min pretreatment with edelfosine completely prevented histamine-induced Ca^{2+} release (Fig. 1*D*), indicating that the ER-Ca^{2+} stores had been depleted during drug treatment. Short drug treatments (≤15 min) were carried out in the microscope chamber while recording calcium changes (upper and medium records) in Ca^{2+}-free (0 Ca^{2+}) medium containing 0.5 mmol/L of EGTA to prevent any possible effect of edelfosine on calcium entry. Some experiments were done in the presence of 0.2 mmol/L of Mn^{2+} as a calcium surrogate rendering identical results (data not shown), thus, ruling out calcium entry in these conditions. When we did longer drug treatments (>30 min), cells were incubated in standard medium with 10 μmol/L of edelfosine to avoid Ca^{2+} store depletion due to protracted incubations in 0 Ca^{2+} medium. Then, cells were mounted in the microscope chamber to measure cytosolic Ca^{2+} as above. In these cases, cells were initially perfused with standard medium, and then with 0 Ca^{2+} medium to stimulate the cells with histamine (Fig. 1*D, bottom left*). We also observed a small increase in the cytosolic calcium baseline with long drug pretreatments, 15 to 60 min (Fig. 1*D, left*; data not shown), indicating that Ca^{2+} stores are being emptied. In time course assays, we found that edelfosine caused a gradual calcium discharge from the ER up to its total depletion in HeLa cells. In Fig. 1*D* (*right*), we represent the amplitude of the calcium peak with histamine as cytoplasmic-free Ca^{2+} concentration (nmol/L) versus the time of edelfosine treatment, showing an exponential decay of histamine-induced calcium release when drug incubation times are increased. These data indicate that edelfosine affects Ca^{2+} homeostasis.

Edelfosine induces ER stress. We next examined the effects of edelfosine on a number of ER stress–associated markers. RT-PCR and immunoblotting analyses showed that edelfosine induced the expression of transcription factor CHOP/GADD153 at both mRNA and protein levels (Fig. 2*A*). The *N*-glycosylation inhibitor tunicamycin was used as a positive control for ER stress (27).

Because ER is not only responsible for protein synthesis, but also for initial posttranslational protein modification, folding and export, disturbances in the ER lead to the accumulation of misfolded proteins. Cells trigger a specific survival signaling in response to ER stress, known as the unfolded protein response (UPR; ref. 13), which mainly involves the expression of Grp78/BiP chaperone, trying to enhance the ER protein folding capacity. Edelfosine did not up-regulate Grp78/BiP (Fig. 2*A*). Thus, these results suggest that edelfosine induces an apoptotic signal without unleashing the typical UPR. In this regard, inhibition of phosphatidylcholine synthesis has been reported to induce CHOP/GADD153 without any change in Grp78/BiP protein levels (28).

Caspase-12 mediates ER stress–induced apoptosis in murine cells, but human cells do not possess a functional caspase-12 gene (29). Because human caspase-4 is a potential homologue of murine caspase-12, we analyzed whether caspase-4 was involved in edelfosine-induced cell death. Caspase-4 was cleaved to its active

form in HeLa cells following protracted incubation times with edelfosine and after the triggering of apoptosis (see Figs. 1*A* and 2*A*). However, caspase-8 and caspase-3 were activated before the onset of the apoptotic response (Fig. 2*A*). BAP31, an integral membrane protein of the ER that is a caspase-8 substrate (30), was cleaved into a p20 fragment following edelfosine treatment (Fig. 2*A*). The p20-BAP31 protein has been shown to direct proapoptotic signals between ER and mitochondria (31).

We also found that preincubation of HeLa cells with the caspase-4 inhibitor z-LEVD-fmk and the caspase-8 inhibitor z-IETD-fmk diminished edelfosine-induced apoptosis by 42% and 65%, respectively (Fig. 2*B, top*), when used at concentrations that

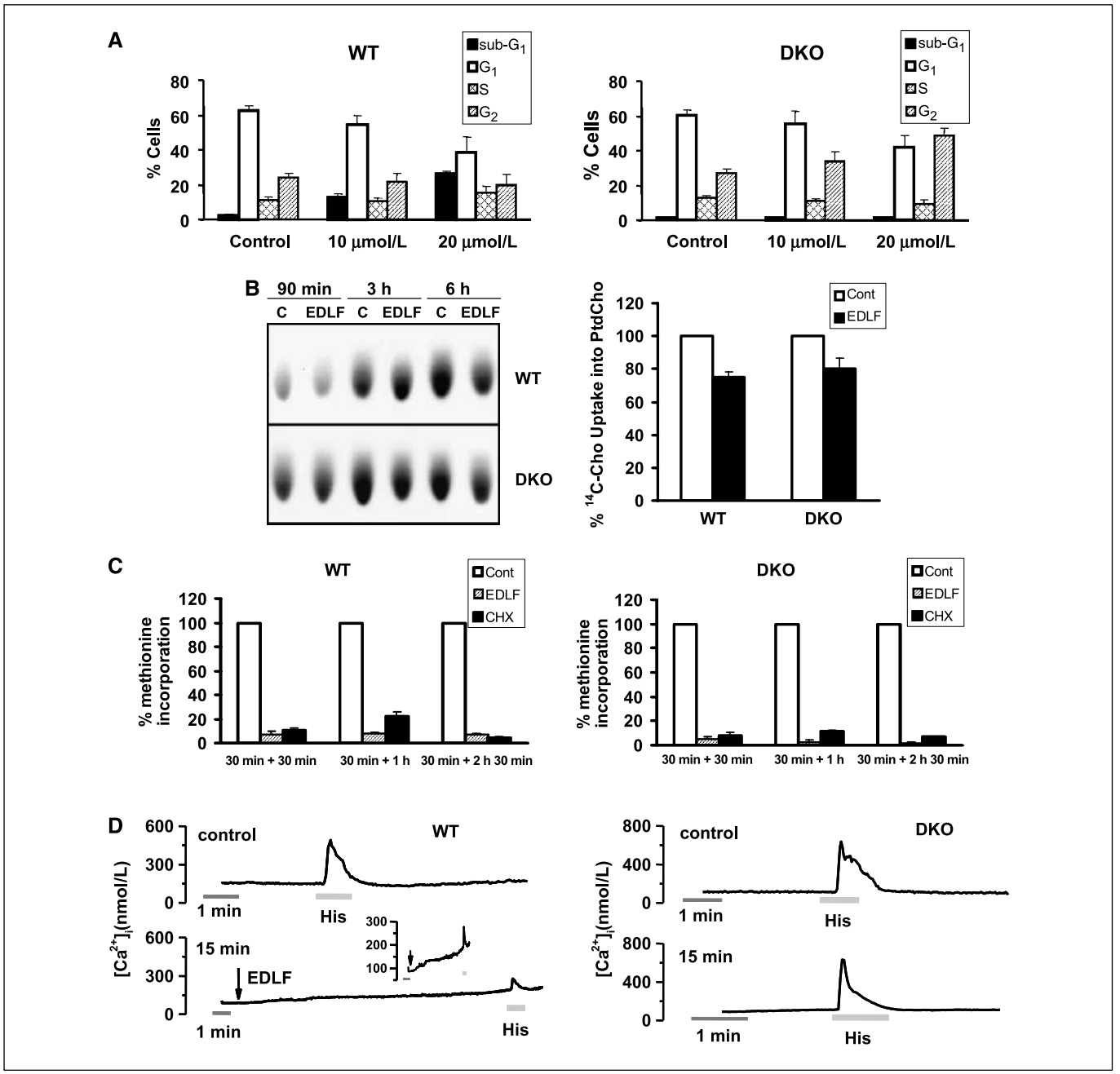

Figure 4. Resistance of DKO cells to edelfosine-induced apoptosis. *A,* wild-type (*WT*) and DKO cells were treated for 24 h with edelfosine at the indicated concentrations. The proportion of cells in each phase of the cell cycle were quantitated by flow cytometry, the sub-G_1 region representing apoptotic cells. Untreated control cells were run in parallel. *Columns,* means; *bars,* SE ($n = 3$). *B, left,* [^{14}C]choline-labeled cells were grown in the absence (*C*) or presence of 20 μmol/L of edelfosine (*EDLF*) for the indicated times. Image shows phosphatidylcholine-corresponding TLC spots visualized by phosphorimaging, and is representative of three independent experiments. *Right,* percentage of [^{14}C]choline (*Cho*) incorporation into phosphatidylcholine (*PtdCho*) in DKO cells treated with 20 μmol/L of edelfosine cells for 6 h (*EDLF*) with respect to untreated control DKO cells (*Cont*; 100%). *Columns,* means; *bars,* SE ($n = 3$). *C,* cells were preincubated for 30 min in the absence (*Cont*) or presence of 20 μmol/L edelfosine (*EDLF*) or 75 μmol/L of cycloheximide (*CHX*), and then [^{35}S]methionine was added to the culture medium for the indicated times. Percentage of newly synthesized labeled proteins in drug-treated cells with respect to untreated samples (100%). *Columns,* means; *bars,* SE ($n = 3$). *D,* cytosolic calcium was measured in fura-2/AM–loaded wild-type (*left*) or DKO (*right*) cells. Calcium release from intracellular stores was elicited by 100 μmol/L of histamine in 0 Ca^{2+} medium in control conditions (*top*) or in the presence of 1 μmol/L of edelfosine (*bottom*) after 15-min incubation. *Inset,* the same record as the bottom left values in an expanded calcium scale.

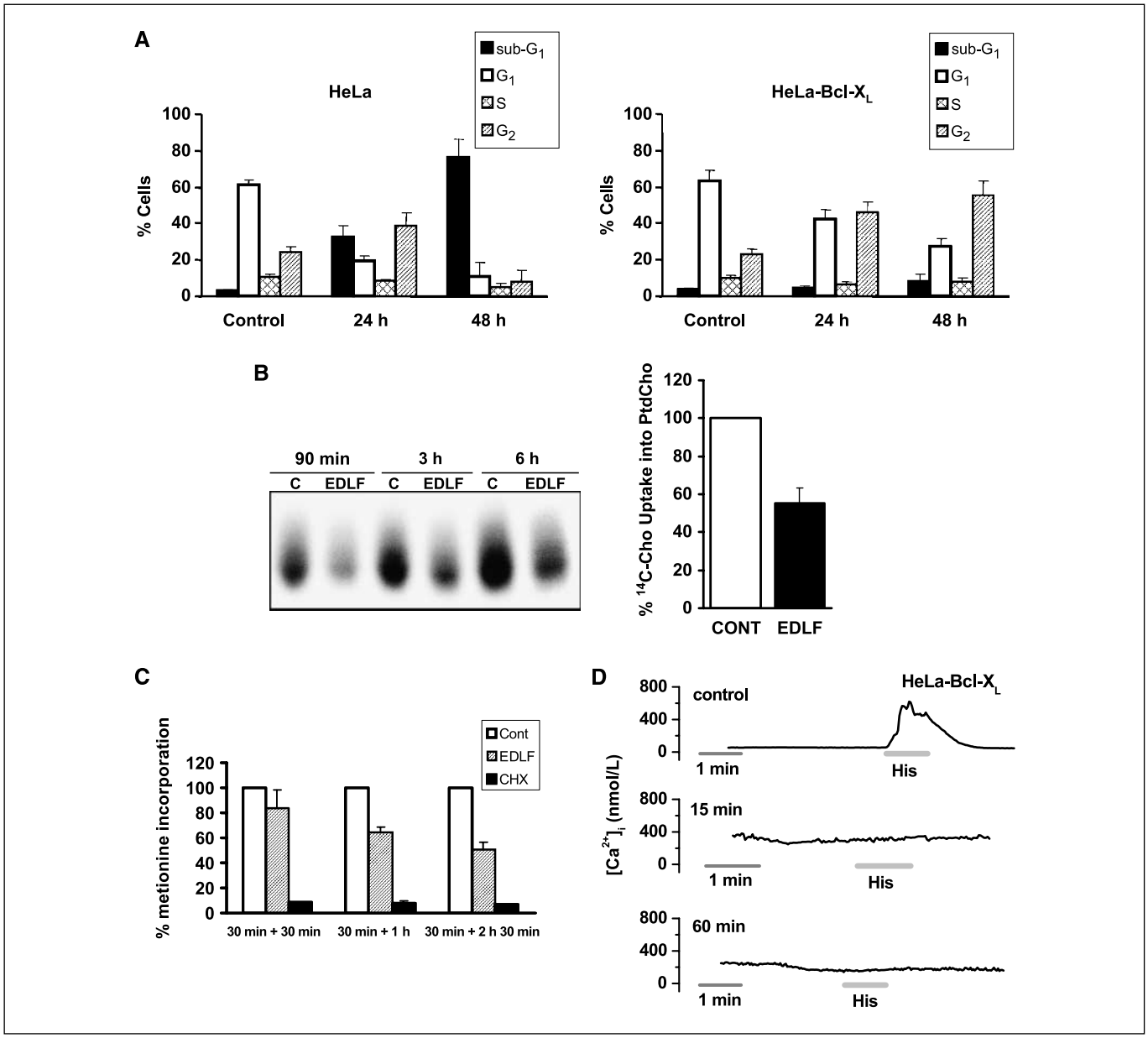

Figure 5. Overexpression of *bcl-x*$_L$ inhibits edelfosine-induced apoptosis. *A,* HeLa and HeLa-Bcl-X$_L$ cells were treated with 10 μmol/L of edelfosine for the indicated times and the proportion of cells in each cell cycle phase was quantitated by flow cytometry. The sub-G$_1$ region represents apoptotic cells. Untreated control cells were run in parallel. *Columns,* means; *bars,* SE (n = 4). *B, left,* [^{14}C]choline-labeled HeLa-Bcl-X$_L$ cells were grown in the absence (*C*) or presence of 10 μmol/L of edelfosine (*EDLF*) for the indicated times. Image shows phosphatidylcholine-corresponding TLC spots visualized by phosphorimaging and is representative of three independent experiments. *Right,* percentage of [^{14}C]choline (*Cho*) incorporation into phosphatidylcholine (*PtdCho*) in HeLa-Bcl-X$_L$ cells treated with 10 μmol/L of edelfosine cells for 6 h (*EDLF*) with respect to untreated HeLa-Bcl-X$_L$ control cells (*CONT*; 100%). *Columns,* means; *bars,* SE (n = 3). *C,* HeLa-Bcl-X$_L$ cells were preincubated for 30 min in the absence (*Cont*) or presence of edelfosine (*EDLF*) or cycloheximide (*CHX*), and then [^{35}S]methionine was added to the culture medium for the indicated times to measure the percentage of newly synthesized labeled proteins with respect to untreated samples (100%). *Columns,* means; *bars,* SE (n = 3). *D,* calcium measurements in fura-2/AM–loaded HeLa-Bcl-X$_L$ cells. Cells were incubated with 10 μmol/L of edelfosine for 15 min in 0 Ca^{2+} medium (*middle*) or for 60 min in medium containing calcium (*bottom*), and calcium release was elicited with 100 μmol/L of histamine in 0 Ca^{2+} medium in both cases as well as in untreated control conditions (*top*). Mean values of >100 cells from four different experiments.

prevented caspase activation (Fig. 2*B, bottom*). Caspase-8 inhibition almost completely abrogated the p20-BAP31 fragment generation (Fig. 2*B, bottom right*). Our data suggest that caspase-4 contributes to the apoptotic response mediated by ER, but it does not participate in the early triggering of apoptosis signaling.

ER stress has been shown to induce the activation of Bax and Bak leading to conformational changes that expose previously NH_2 terminus–occluded regions in their corresponding nonactive forms (32). Activation of these proapoptotic Bcl-2 family members can be detected by using anti-Bax (clone 6A7) and anti-Bak (clone Ab-1) monoclonal antibodies that recognize the NH_2-terminal epitopes of human Bax and Bak, respectively, and thereby their corresponding active forms. These antibodies have been previously used to show the activation of Bax and Bak in response to distinct apoptotic stimuli (32, 33). Interestingly, edelfosine treatment induced an increase in the Bax protein expression level, without affecting the

protein levels of Bak and of the antiapoptotic Bcl-2 family member Bcl-X_L (Fig. 2*C*). We also found that treatment of HeLa cells with edelfosine promoted a significant activation of Bax, whereas Bak was weakly activated (Fig. 2*D*).

ASK1-mediated JNK activation in edelfosine-induced apoptosis. Previous studies indicate that ASK1-mediated JNK activation is crucial for ER-induced apoptosis (14). Edelfosine has been reported to induce persistent JNK activation before the onset of apoptosis (7). Pretreatment of HeLa cells with the specific JNK inhibitor SP600125 reduced edelfosine-induced JNK activation and apoptosis (Fig. 3*A*). We stably transfected HeLa cells with wild-type ASK1 (Fig. 3*B*) and found that ASK1 overexpression enhanced edelfosine-induced JNK activation (Fig. 3*C*) and cell death (Fig. 3*D*). These data are in concordance with the notion that ASK1/JNK signaling is involved in ER stress–induced apoptosis.

Absence of Bax and Bak inhibits edelfosine-induced apoptosis. Although the function of Bcl-2 family proteins is best characterized at the mitochondrion, some of these proteins also localize to the ER affecting its membrane permeability and regulating apoptosis (32). ER stress responses induce conformational changes and oligomerization of Bax and Bak on the ER, initiating apoptosis (32), and $bax^{-/-}bak^{-/-}$ DKO MEFs are resistant to ER stress–mediated apoptosis (20). DKO cells were completely resistant to edelfosine even when used at high concentrations (Fig. 4*A*; Supplementary Fig. S2*A* and *B*) and showed an accumulation of cells in G_2-M phase following edelfosine treatment (Fig. 4*A*; Supplementary Fig. S2*B*). Edelfosine induced apoptosis at a similar extent in wild-type MEFs and MEFs individually deficient in either Bax or Bak, requiring the absence of both Bax and Bak to prevent cell death (Supplementary Fig. S2*A*). This is in agreement with the redundant roles of Bax and Bak on apoptosis, entailing the knockdown of both proteins to abrogate ER stress–mediated apoptosis (34).

Phosphatidylcholine was weakly and similarly inhibited in either wild-type or DKO cells (Fig. 4*B*). Edelfosine inhibited protein biosynthesis in both wild-type and DKO cells (Fig. 4*C*). These data suggest that inhibition of phosphatidylcholine and protein biosynthesis is not critical for the apoptotic response triggered by edelfosine.

Overexpression of Bax and Bak promotes Ca^{2+} mobilization from the ER to the mitochondria during apoptosis (35). Bax and Bak have been shown to alter Ca^{2+} homeostasis in response to ER stress (34). On these grounds, we analyzed the ER-stored Ca^{2+} depletion in wild-type versus DKO cells following edelfosine treatment. We found that incubation of wild-type MEFs with edelfosine led to an almost total depletion of ER-stored Ca^{2+} after 15 min of incubation (Fig. 4*D, left*). Cells were perfused with 0 Ca^{2+} medium containing 1 μmol/L of edelfosine and then stimulated with 100 μmol/L of histamine. Calcium release in this condition was 73% smaller than in control edelfosine-free conditions. Edelfosine was used at 1 μmol/L because MEFs were detached at higher drug concentrations. Calcium was gradually increased in the cytosol, being slowly released from the Ca^{2+} stores upon edelfosine incubation (see inset in Fig. 4*D, left*). However, the absence of Bax and Bak in DKO cells blocked edelfosine-induced ER-stored Ca^{2+} depletion, and thereby, Ca^{2+} could be released by histamine (Fig. 4*D, right*). Edelfosine failed to promote Ca^{2+} release in DKO cells even after 60 min of incubation (data not shown). These data suggest that edelfosine-induced apoptosis is dependent on Bax/Bak-mediated Ca^{2+} release from ER.

Bcl-X_L overexpression protects cells from edelfosine-induced apoptosis. To study the role of mitochondria in edelfosine-induced cell death, we stably transfected HeLa cells with the expression vector pSFFV-*bcl-x_L*, containing the human *bcl-x_L* open reading frame, or with control pSFFV-Neo plasmid. HeLa cells transfected with the pSFFV-Neo plasmid behaved similarly to wild-type HeLa cells (data not shown). HeLa cells expressed endogenous Bcl-X_L, but Western blot analysis showed a much higher expression of Bcl-X_L protein in *bcl-x_L*–transfected HeLa cells (Supplementary Fig. S3*A*). Gene transfer–mediated overexpression of Bcl-X_L prevented apoptosis in edelfosine-treated HeLa cells (Fig. 5*A*). Bcl-X_L–transfected HeLa cells were accumulated in the G_2-M phase following edelfosine treatment (Fig. 5*A*), and after 4 days of incubation, most of the cells were arrested in G_2-M phase without induction of apoptosis (Supplementary Fig. S3*B*). Edelfosine inhibited both phosphatidylcholine and protein synthesis in Bcl-X_L–transfected HeLa cells (Fig. 5*B* and *C*), similarly to wild-type HeLa cells (Fig. 1*B* and *C*). Edelfosine caused a total calcium discharge from the ER of Bcl-X_L–transfected HeLa cells (Fig. 5*D*), an effect that is similar to that observed in wild-type HeLa cells (Fig. 1*D*). The middle and bottom traces of Fig. 5*D* show that the basal calcium levels are higher in edelfosine-treated cells than in untreated control cells (300 versus 100 nmol/L Ca^{2+}), which is compatible with Ca^{2+} being released from the ER. Because Bcl-X_L protein specifically localizes and acts on mitochondria (36), our results suggest that the apoptotic signals triggered by edelfosine at the ER converge on the mitochondria.

Discussion

Here, we report for the first time that the ALP prototype edelfosine affects ER functions which lead to ER stress and apoptosis in human solid tumor cells. Edelfosine promotes a number of changes in ER-regulated homeostatic processes leading to the triggering of sundry ER-derived apoptotic events that eventually converge on the mitochondria.

Edelfosine inhibits phosphatidylcholine synthesis in solid tumor cells. Previous reports have shown that phosphatidylcholine biosynthesis is blocked by edelfosine through the inhibition of CCT (25). CCT catalyzes the rate-limiting step in *de novo* phosphatidylcholine synthesis in higher animal cells, and its activity is modulated by the stored curvature strain energy in lipid membranes (37). Class II lipids, like diacylglycerol and unsaturated phosphatidylethanolamines, tend to form aggregates in which the polar/apolar interface bends toward the polar environment leading to a curvature disposition. The flattening of these lipids at the cell membrane leads to a stored curvature elastic strain that is released by the partitioning of CCT into the membrane, and thereby, class II lipids activate CCT. By contrast, class I lipids, such as ALPs, are characterized by their ability to form aggregates in which the polar/apolar interface curves away from the polar region and inhibit CCT (37, 38). However, the similar patterns of phosphatidylcholine inhibition observed in both sensitive HeLa cells and drug-resistant Bcl-X_L–transfected cells as well as in wild-type and drug-resistant $bax^{-/-}bak^{-/-}$ DKO cells suggest that phosphatidylcholine inhibition is not essential for the apoptotic cell death induced by edelfosine. This is in agreement with recent evidence showing that the inhibition of phosphatidylcholine synthesis is not the primary pathway in the induction of apoptosis by the ALP hexadecylphosphocholine, as assessed by comparison of hexadecylphosphocholine-induced apoptosis in CHO cells versus

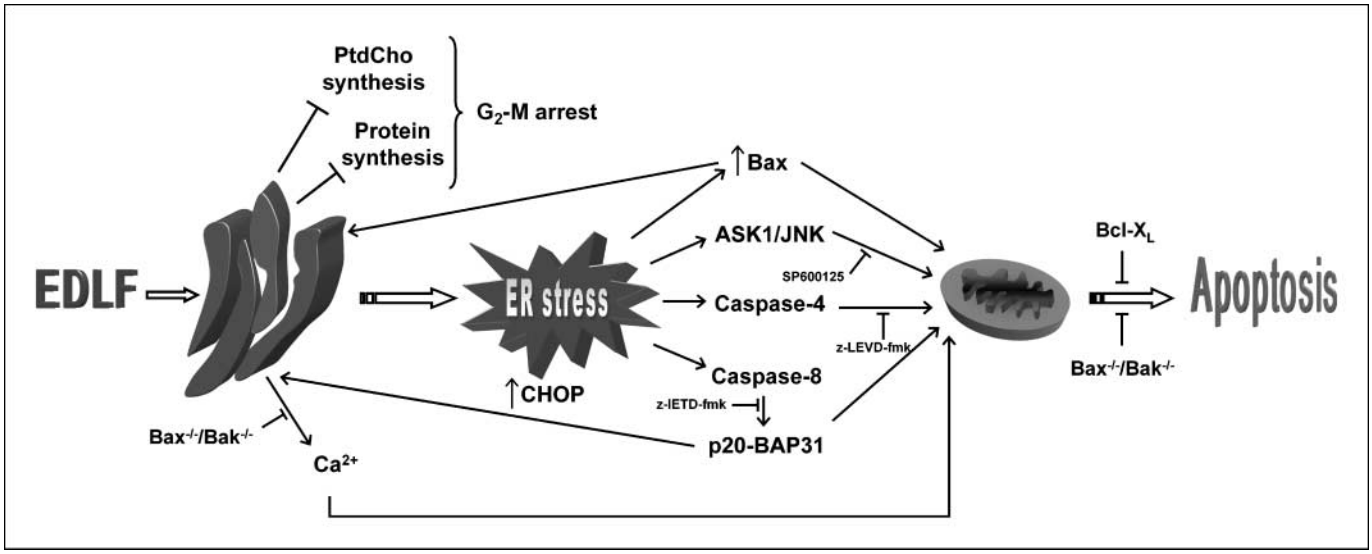

Figure 6. Schematic model of ER involvement in edelfosine-induced apoptosis. This is a schematic diagram designed to portray one currently plausible mechanism of how edelfosine induces apoptosis via ER stress. Edelfosine is incorporated into the tumor cell and accumulates in the ER, leading to the inhibition of phosphatidylcholine (*PtdCho*) and protein synthesis, and to G_2-M arrest. Edelfosine also induces Bax/Bak-mediated ER-stored Ca^{2+} depletion, Bax up-regulation and activation, CHOP/GADD153 up-regulation, ASK1-dependent JNK-persistent activation, and caspase-4 and caspase-8 activation with the generation of the p20-BAP31 fragment. All of these events may lead to apoptosis through a mitochondrial-dependent process. The caspase inhibitors z-LEVD-fmk and z-IETD-fmk, and the JNK inhibitor SP600125, reduce, only in part, the edelfosine-induced apoptosis, suggesting that these processes are acting in parallel. Protection of mitochondria by Bcl-X_L overexpression fully restrains cell death, indicating that the ER-triggered apoptotic signaling pathways converge on the mitochondria.

CHO-MT58 cells that contain a genetic defect in CCT and phosphatidylcholine synthesis (39). Likewise, farnesol-induced apoptosis has also been shown to be uncoupled from farnesol-mediated inhibition of phosphatidylcholine biosynthesis (40). Edelfosine has also been reported to inhibit phosphatidylcholine synthesis at a similar rate in both sensitive MCF-7 and resilient A549 tumor cell lines, A549 cell proliferation being unaffected (41). Hexadecylphosphocholine-induced apoptosis is prevented by the addition of either lysophosphatidylethanolamine or lysophosphatidylcholine, despite the fact that only lysophosphatidylcholine is able to attenuate the effect of the drug on phosphatidylcholine synthesis (39). This suggests that a more general disturbance in membrane structure, rather than a specific alteration in phosphatidylcholine metabolism, underlies ALP-induced apoptosis (39). In this regard, edelfosine accumulates in lipid rafts (10, 42), modifying membrane lipid composition and protein function (43). Thus, ALPs could induce a general disturbance in the membrane structure or bilayer packing, which may lead to membrane leakage or destabilization.

The results reported here indicate that edelfosine inhibits protein synthesis, a hallmark of ER stress. UPR is triggered as a cellular survival response to ER stress. The balance between Grp78/BiP, a UPR hallmark, and CHOP/GADD153 expression is considered to lead to either cell survival or cell death in ER stress. Less susceptibility to cell death upon activation of the UPR may contribute to the tumor progression of solid tumors. Here, we found that edelfosine induced CHOP/GADD153 expression, whereas Grp78/BiP protein levels remained unaffected, tipping the balance in favor of an ER stress–induced cell death. Our study shows that edelfosine induces a number of ER stress markers, including CHOP/GADD153 up-regulation. Interestingly, Fas/CD95 death receptor is involved in the antitumor action of edelfosine in tumor cells (5, 9, 10, 21), and Fas/CD95-induced apoptosis has been reported to be mediated by CHOP/GADD153 (44). Thus, a putative link between Fas/CD95 and ER could be envisaged in the action of edelfosine in cancer cells. In addition, the accumulation of edelfosine in lipid rafts (10, 42), together with the edelfosine-induced coclustering of Fas/CD95 in lipid rafts in leukemic cells (5, 9, 10, 45), and recent evidence suggesting the existence of lipid rafts in the ER (46, 47), might link the involvement of lipid rafts and ER in the antitumor action of edelfosine.

Our data suggest that edelfosine-induced JNK activation is mediated by ASK1. Caspase-4 was activated after the onset of apoptosis in edelfosine-treated HeLa cells, suggesting that caspase-4 enhances the apoptotic response, but it is not required for the triggering of cell death. These data square with recent evidence showing that caspase-4 activation detected in ER stress–induced apoptosis is not the result of an initiating event, but it occurs further downstream in the apoptotic cascade (48). However, caspase-8 and caspase-3 were activated before the onset of apoptosis following edelfosine treatment. Caspase-8 cleavage of BAP31 at the ER leads to the generation of a p20 fragment that directs proapoptotic signals between ER and mitochondria, resulting in an early discharge of Ca^{2+} from the ER and its concomitant uptake into the mitochondria, which prompts mitochondrial fission and cytochrome *c* release to the cytosol (31). Our present data show that edelfosine induces the cleavage of BAP31 with the formation of proapoptotic p20 fragment and causes a gradual ER-stored Ca^{2+} release up to its total depletion in HeLa cells. Edelfosine-induced apoptosis and ER-stored Ca^{2+} discharge were totally prevented in DKO cells. These data suggest that edelfosine-induced apoptosis is dependent on Bax/Bak-mediated Ca^{2+} release. Thus, our results indicate that Ca^{2+} signaling is essential for the mechanism of action of edelfosine, likely regulating the link between ER and mitochondria, and in this way, influencing the sensitivity of mitochondria to other stress signals. Overexpression of Bcl-X_L, which specifically localizes and acts on the mitochondria (36), blocks the apoptotic response induced by edelfosine without affecting G_2-M arrest or Ca^{2+} discharge from the ER. This indicates that the

apoptotic signals set off by edelfosine at the ER converge on the mitochondria.

Our data from wild-type and DKO cells indicate that edelfosine inhibition of phosphatidylcholine and protein biosynthesis is not critical for the apoptotic response induced by edelfosine and is independent of the mechanism related with Bax/Bak. Edelfosine treatment leads to a conformational change of Bax. This conformational change has been coupled to its activation and precedes Bax translocation to the mitochondria and/or ER, which may lead to a lesion of the organelle membrane integrity (32, 49). In addition, edelfosine increased the protein levels of Bax, whereas the protein levels of the antiapoptotic Bcl-X_L and proapoptotic Bak were not altered. Thus, the accumulation of edelfosine in the ER leads to Bax activation and to higher levels of Bax protein level, suggesting a major role for Bax in the edelfosine-induced apoptotic response. Our previous (1) and present data indicate that edelfosine does not modify the expression of antiapoptotic *Bcl-2* and *Bcl-X_L* genes, whereas Bax is up-regulated. Thus, the ratio of antiapoptotic to proapoptotic molecules such as Bcl-2 or Bcl-X_L/Bax, which constitutes a rheostat that sets the threshold of susceptibility to apoptosis, is shifted in favor of apoptosis induction following edelfosine treatment. The apparent lack of significant activation of Bak in drug-treated cells, despite the fact that cells deficient in both *bax/bak* are required for edelfosine resistance, might be due to either a faulty experimental approach to detect the appropriate activating Bak conformational change or to a rather different and complex regulation of Bak in apoptosis that involves the preexistence and alteration of several protein complexes (50).

Figure 6 depicts a model for the involvement of ER in edelfosine-induced apoptosis in solid tumor cells based on our current data. Unlike several anticancer drugs that induce ER stress in an indirect way, edelfosine accumulates in the ER of solid tumor cells (11). This drug accumulation leads first to the inhibition of phosphatidylcholine and protein synthesis by inhibiting CCT and promoting eIF2α phosphorylation. These events promote G_2-M arrest, but fail to induce per se an apoptotic response. In addition, edelfosine induces Bax/Bak-mediated ER-stored Ca^{2+} depletion, Bax up-regulation and activation, CHOP/GADD153 up-regulation, caspase-4 and caspase-8 activation, p20-BAP31 fragment generation, and ASK1-dependent JNK-persistent activation. The fact that prevention of caspase-8, caspase-4, or JNK activation inhibits only in part edelfosine-induced apoptosis indicates that these processes are triggered in a rather parallel way. In contrast, Bcl-X_L overexpression totally blocks cell death, indicating that these parallel apoptotic pathways converge on the mitochondria as the ultimate step to rendering an apoptotic outcome. Our data on the ER Ca^{2+} release exerted by edelfosine in wild-type cells, but not in $bax^{-/-}bak^{-/-}$ doubly deficient cells, suggests that Bax and Bak play an important role in the proapoptotic mechanism of the drug, involving the release of the ER Ca^{2+} pool with subsequent sensitization of mitochondria. Taken together, our findings indicate that accumulation of edelfosine in the ER results in profound alterations of the organelle functions, followed by transcriptional and biochemical changes that eventually lead to apoptosis through a mitochondrion-mediated process.

Acknowledgments

Received 1/25/2007; revised 7/31/2007; accepted 9/6/2007.

Grant support: Fondo de Investigación Sanitaria and European Commission (FIS-FEDER 06/0813, 04/0843, 04/0789, 03/0975, 02/1199), Ministerio de Educación y Ciencia (SAF2005-04293, BFU2005-05464), Fundación de Investigación Médica Mutua Madrileña, Fundación "la Caixa" (BM05-30-0), and Junta de Castilla y León (CSI04A05). T. Nieto-Miguel is the recipient of a predoctoral fellowship from the Junta de Castilla y León, L. Vay is the recipient of a predoctoral fellowship from the Fondo de Investigación Sanitaria, and C. Gajate is supported by the Ramón y Cajal Program from the Ministerio de Educación y Ciencia of Spain.

The costs of publication of this article were defrayed in part by the payment of page charges. This article must therefore be hereby marked *advertisement* in accordance with 18 U.S.C. Section 1734 solely to indicate this fact.

References

1. Mollinedo F, Fernandez-Luna JL, Gajate C, et al. Selective induction of apoptosis in cancer cells by the ether lipid ET-18-OCH_3 (Edelfosine): molecular structure requirements, cellular uptake, and protection by Bcl-2 and Bcl-X_L. Cancer Res 1997;57:1320–8.
2. Gajate C, Mollinedo F. Biological activities, mechanisms of action and biomedical prospect of the antitumor ether phospholipid ET-18-OCH_3 (Edelfosine), a proapoptotic agent in tumor cells. Curr Drug Metab 2002;3:491–525.
3. Mollinedo F, Gajate C, Martin-Santamaria S, Gago F. ET-18-OCH_3 (edelfosine): a selective antitumour lipid targeting apoptosis through intracellular activation of Fas/CD95 death receptor. Curr Med Chem 2004;11:3163–84.
4. Hideshima T, Catley L, Yasui H, et al. Perifosine, an oral bioactive novel alkylphospholipid, inhibits Akt and induces *in vitro* and *in vivo* cytotoxicity in human multiple myeloma cells. Blood 2006;107:4053–62.
5. Gajate C, Mollinedo F. Edelfosine and perifosine induce selective apoptosis in multiple myeloma by recruitment of death receptors and downstream signaling molecules into lipid rafts. Blood 2007;109:711–9.
6. Mollinedo F, Martinez-Dalmau R, Modolell M. Early and selective induction of apoptosis in human leukemic cells by the alkyl-lysophospholipid ET-18-OCH_3. Biochem Biophys Res Commun 1993;192:603–9.
7. Gajate C, Santos-Beneit A, Modolell M, Mollinedo F. Involvement of c-Jun NH2-terminal kinase activation and c-Jun in the induction of apoptosis by the ether phospholipid 1-*O*-octadecyl-2-*O*-methyl-*rac*-glycero-3-phosphocholine. Mol Pharmacol 1998;53:602–12.
8. Gajate C, Santos-Beneit AM, Macho A, et al. Involvement of mitochondria and caspase-3 in ET-18-OCH_3-induced apoptosis of human leukemic cells. Int J Cancer 2000;86:208–18.
9. Gajate C, Mollinedo F. The antitumor ether lipid ET-18-OCH_3 induces apoptosis through translocation and capping of Fas/CD95 into membrane rafts in human leukemic cells. Blood 2001;98:3860–3.
10. Gajate C, Del Canto-Janez E, Acuna AU, et al. Intracellular triggering of Fas aggregation and recruitment of apoptotic molecules into Fas-enriched rafts in selective tumor cell apoptosis. J Exp Med 2004;200:353–65.
11. Nieto-Miguel T, Gajate C, Mollinedo F. Differential targets and subcellular localization of antitumor alkyl-lysophospholipid in leukemic versus solid tumor cells. J Biol Chem 2006;281:14833–40.
12. Rao RV, Ellerby HM, Bredesen DE. Coupling endoplasmic reticulum stress to the cell death program. Cell Death Differ 2004;11:372–80.
13. Kim R, Emi M, Tanabe K, Murakami S. Role of the unfolded protein response in cell death. Apoptosis 2006;11:5–13.
14. Nishitoh H, Matsuzawa A, Tobiume K, et al. ASK1 is essential for endoplasmic reticulum stress-induced neuronal cell death triggered by expanded polyglutamine repeats. Genes Dev 2002;16:1345–55.
15. Hitomi J, Katayama T, Eguchi Y, et al. Involvement of caspase-4 in endoplasmic reticulum stress-induced apoptosis and Abeta-induced cell death. J Cell Biol 2004;165:347–56.
16. Fribley A, Zeng Q, Wang CY. Proteasome inhibitor PS-341 induces apoptosis through induction of endoplasmic reticulum stress-reactive oxygen species in head and neck squamous cell carcinoma cells. Mol Cell Biol 2004;24:9695–704.
17. Mimnaugh EG, Xu W, Vos M, et al. Simultaneous inhibition of hsp 90 and the proteasome promotes protein ubiquitination, causes endoplasmic reticulum-derived cytosolic vacuolization, and enhances antitumor activity. Mol Cancer Ther 2004;3:551–66.
18. Mandic A, Hansson J, Linder S, Shoshan MC. Cisplatin induces endoplasmic reticulum stress and nucleus-independent apoptotic signaling. J Biol Chem 2003;278:9100–6.
19. Carracedo A, Gironella M, Lorente M, et al. Cannabinoids induce apoptosis of pancreatic tumor cells via endoplasmic reticulum stress-related genes. Cancer Res 2006;66:6748–55.
20. Wei MC, Zong WX, Cheng EH, et al. Proapoptotic BAX and BAK: a requisite gateway to mitochondrial dysfunction and death. Science 2001;292:727–30.
21. Gajate C, Fonteriz RI, Cabaner C, et al. Intracellular triggering of Fas, independently of FasL, as a new mechanism of antitumor ether lipid-induced apoptosis. Int J Cancer 2000;85:674–82.
22. Gajate C, Barasoain I, Andreu JM, Mollinedo F. Induction of apoptosis in leukemic cells by the reversible microtubule-disrupting agent 2-methoxy-5-(2′,3′,4′-trimethoxyphenyl)-2,4,6-cycloheptatrien-1-one: protection by Bcl-2 and Bcl-X_L and cell cycle arrest. Cancer Res 2000;60:2651–9.

23. Grynkiewicz G, Poenie M, Tsien RY. A new generation of Ca^{2+} indicators with greatly improved fluorescence properties. J Biol Chem 1985;260: 3440–50.
24. Hoffman DR, Thomas VL, Snyder F. Inhibition of cellular transport systems by alkyl phospholipid analogs in HL-60 human leukemia cells. Biochim Biophys Acta 1992;1127:74–80.
25. Boggs KP, Rock CO, Jackowski S. Lysophosphatidylcholine and 1-*O*-octadecyl-2-*O*-methyl-*rac*-glycero-3-phosphocholine inhibit the CDP-choline pathway of phosphatidylcholine synthesis at the CTP:phosphocholine cytidylyltransferase step. J Biol Chem 1995;270: 7757–64.
26. Samuel CE. The eIF-2 α protein kinases, regulators of translation in eukaryotes from yeasts to humans. J Biol Chem 1993;268:7603–6.
27. Liu H, Bowes RC III, van de Water B, Sillence C, Nagelkerke JF, Stevens JL. Endoplasmic reticulum chaperones GRP78 and calreticulin prevent oxidative stress, Ca2+ disturbances, and cell death in renal epithelial cells. J Biol Chem 1997;272:21751–9.
28. van der Sanden MH, Houweling M, van Golde LM, Vaandrager AB. Inhibition of phosphatidylcholine synthesis induces expression of the endoplasmic reticulum stress and apoptosis-related protein CCAAT/enhancer-binding protein-homologous protein (CHOP/GADD153). Biochem J 2003;369:643–50.
29. Saleh M, Vaillancourt JP, Graham RK, et al. Differential modulation of endotoxin responsiveness by human caspase-12 polymorphisms. Nature 2004;429:75–9.
30. Ng FW, Nguyen M, Kwan T, et al. p28 Bap31, a Bcl-2/Bcl-XL- and procaspase-8-associated protein in the endoplasmic reticulum. J Cell Biol 1997;139:327–38.
31. Breckenridge DG, Stojanovic M, Marcellus RC, Shore GC. Caspase cleavage product of BAP31 induces mitochondrial fission through endoplasmic reticulum calcium signals, enhancing cytochrome c release to the cytosol. J Cell Biol 2003;160:1115–27.
32. Zong WX, Li C, Hatzivassiliou G, et al. Bax and Bak can localize to the endoplasmic reticulum to initiate apoptosis. J Cell Biol 2003;162:59–69.
33. Griffiths GJ, Dubrez L, Morgan CP, et al. Cell damage-induced conformational changes of the pro-apoptotic protein Bak *in vivo* precede the onset of apoptosis. J Cell Biol 1999;144:903–14.
34. Scorrano L, Oakes SA, Opferman JT, et al. BAX and BAK regulation of endoplasmic reticulum Ca2+: a control point for apoptosis. Science 2003;300:135–9.
35. Nutt LK, Pataer A, Pahler J, et al. Bax and Bak promote apoptosis by modulating endoplasmic reticular and mitochondrial Ca^{2+} stores. J Biol Chem 2002;277: 9219–25.
36. Kaufmann T, Schlipf S, Sanz J, Neubert K, Stein R, Borner C. Characterization of the signal that directs Bcl-x_L, but not Bcl-2, to the mitochondrial outer membrane. J Cell Biol 2003;160:53–64.
37. Davies SM, Epand RM, Kraayenhof R, Cornell RB. Regulation of CTP: phosphocholine cytidylyltransferase activity by the physical properties of lipid membranes: an important role for stored curvature strain energy. Biochemistry 2001;40:10522–31.
38. Attard GS, Templer RH, Smith WS, Hunt AN, Jackowski S. Modulation of CTP:phosphocholine cytidylyltransferase by membrane curvature elastic stress. Proc Natl Acad Sci U S A 2000;97:9032–6.
39. van der Sanden MH, Houweling M, Duijsings D, Vaandrager AB, van Golde LM. Inhibition of phosphatidylcholine synthesis is not the primary pathway in hexadecylphosphocholine-induced apoptosis. Biochim Biophys Acta 2004;1636:99–107.
40. Wright MM, Henneberry AL, Lagace TA, Ridgway ND, McMaster CR. Uncoupling farnesol-induced apoptosis from its inhibition of phosphatidylcholine synthesis. J Biol Chem 2001;276:25254–61.
41. Zhou X, Arthur G. Effect of 1-*O*-octadecyl-2-*O*-methyl-glycerophosphocholine on phosphatidylcholine and phosphatidylethanolamine synthesis in MCF-7 and A549 cells and its relationship to inhibition of cell proliferation. Eur J Biochem 1995;232:881–8.
42. van der Luit AH, Budde M, Ruurs P, Verheij M, van Blitterswijk WJ. Alkyl-lysophospholipid accumulates in lipid rafts and induces apoptosis via raft-dependent endocytosis and inhibition of phosphatidylcholine synthesis. J Biol Chem 2002;277:39541–7.
43. Zaremberg V, Gajate C, Cacharro LM, Mollinedo F, McMaster CR. Cytotoxicity of an anti-cancer lysophospholipid through selective modification of lipid raft composition. J Biol Chem 2005;280: 38047–58.
44. Brenner B, Koppenhoefer U, Weinstock C, Linderkamp O, Lang F, Gulbins E. Fas- or ceramide-induced apoptosis is mediated by a Rac1-regulated activation of Jun N-terminal kinase/p38 kinases and GADD153. J Biol Chem 1997;272:22173–81.
45. Mollinedo F, Gajate C. Fas/CD95 death receptor and lipid rafts: new targets for apoptosis-directed cancer therapy. Drug Resist Updat 2006;9:51–73.
46. Alfalah M, Wetzel G, Fischer I, et al. A novel type of detergent-resistant membranes may contribute to an early protein sorting event in epithelial cells. J Biol Chem 2005;280:42636–43.
47. Browman DT, Resek ME, Zajchowski LD, Robbins SM. Erlin-1 and erlin-2 are novel members of the prohibitin family of proteins that define lipid-raft-like domains of the ER. J Cell Sci 2006; 119:3149–60.
48. Obeng EA, Boise LH. Caspase-12 and caspase-4 are not required for caspase-dependent endoplasmic reticulum stress-induced apoptosis. J Biol Chem 2005;280: 29578–87.
49. Lalier L, Cartron PF, Juin P, et al. Bax activation and mitochondrial insertion during apoptosis. Apoptosis 2007;12:887–96.
50. Chandra D, Choy G, Daniel PT, Tang DG. Bax-dependent regulation of Bak by voltage-dependent anion channel 2. J Biol Chem 2005;280:19051–61.

Endoplasmic Reticulum Stress in the Proapoptotic Action of Edelfosine in Solid Tumor Cells

Teresa Nieto-Miguel, Rosalba I. Fonteriz, Laura Vay, et al.

Cancer Res 2007;67:10368-10378.